

### Structure characterization of the optical reactive spiro-pentacopper cluster : $K_2Cu_5(pGlu)_6(OH)_2 \cdot 10H_2O$

S. M. Chen<sup>1</sup>(15410), I. J.Hsu<sup>1</sup>(6948), Y. C. Lin<sup>1</sup>(9079), Y. Wang<sup>1\*</sup>(6950), J. J. Lee<sup>2</sup>(6947)

<sup>1</sup>Department of Chemistry, National Taiwan University, Taipei 106, Taiwan, R.O.C.  
<sup>2</sup>Synchrotron Radiation Research Center, Hsinchu, Taiwan, R.O.C.

The optical reactive spiro-pentacopper cluster,  $K_2Cu_5(pGlu)_6(OH)_2 \cdot 10H_2O$  has been synthesized and the temperature dependent magnetic susceptibility measurement shows that it undergoes a gradual spin transition from  $\mu_{eff} = 4.442(B.M.)$  at room temperature to  $\mu_{eff} = 2.041(B.M.)$  at low temperature, 5 K, shown in Figure 1. This phenomenon maybe due to the change in spin-coupling between metal centers at various temperature. In order to see if there is any structural change accompanied with the magnetic behavior. The powder diffraction data at two temperatures, 298 K and 9 K, were measured. Using the beamline BL12B1 at Spring-8.

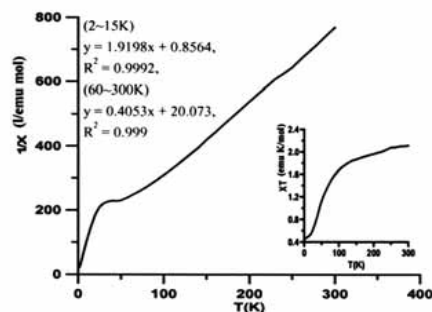


Figure 1. Thermal dependence of  $X_m T$  of compound  $K_2Cu_5(pGlu)_6(OH)_2 \cdot 10H_2O$

The main purposes of this study are (1) to do zero-point shift calibration curve of IP using standard compound  $LaB_6$  with wavelength  $1.4586 \text{ \AA}$  at room temperature (2) to collect room temperature (298 K) and low temperature (9 K) powder data of this optically active spiro-pentacopper cluster,  $K_2Cu_5(pGlu)_6(OH)_2 \cdot 10H_2O$ , for structure determination. Following is a short summary of the present results.

The angle dependent of zero-point shift of  $LaB_6$  is displayed in the Figure 2. Using the polynomial, fitting result  $\Delta 2\theta = -0.003 - 0.08*(2\theta) + 0.095*(2\theta)^2 - 0.02*(2\theta)^3$ , to correct the shift of  $K_2Cu_5(pGlu)_6(OH)_2 \cdot 10H_2O$

powder diffraction data. The corrected powder pattern of spiro-pentacopper cluster at 298K and 9K is shown in Figure 3. The present instrumental resolution is about  $0.02^\circ$  limited by the IP reader. The peak shift observed between two different temperature powder patterns. The higher angle of  $2\theta$  is, the bigger the peak-shift there is. It is consistent with the lattice change. From the relative intensities, it is believed there is no structure change accompanied with the magnetic behavior.

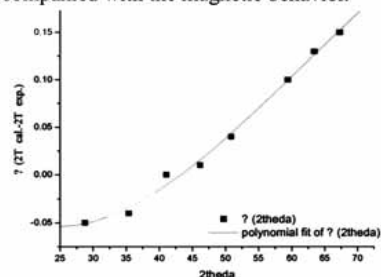


Figure 2. Angle dependent of zero-point shift. Using  $LaB_6$  with  $\lambda=1.4586 \text{ \AA}$ . The square points (■) are the differences between standard and experimental data. The solid line (—) is the fitting result.

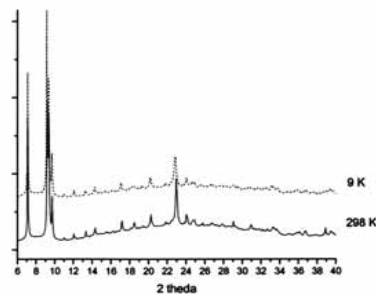


Figure 3. Powder pattern of  $K_2Cu_5(pGlu)_6(OH)_2 \cdot 10H_2O$  at 298 K (—) and 9 K (---) with  $\lambda=1.4586 \text{ \AA}$ .

The Rietveld refinement was performed by using GSAS program. The refinement is still in process.

### Data Collection of Lectin-like Protein from *Oryza sativa*

Yin-Cheng Hsieh<sup>1,2</sup> (0094), Chuen-Yuan Kuo<sup>1,2</sup> (0015647), Chun-Jung Chen<sup>1</sup> (6903)

1. Biology Group, National Synchrotron Radiation Research Center, Hsinchu, Taiwan  
 2. Institute of Bioinformatics and Structural Biology, National Tsing-Hua University, Hsinchu, Taiwan

The rice (*Oryza sativa*) lectin belongs to the subgroup of mannose-binding jacalin-related lectins that can recognize and bind to sugar complexes. Lectins play a role in recognition of certain sugar residues and they can discriminate the carbohydrates found on self glycoproteins and glycolipid from the carbohydrate patterns found on infectious non-self surfaces and perform defense behavior. In addition to the relationship with innate immune system, lectins are used to target and deliver drugs to their site of action. The ideal of this method is that different cell types express different glycan patterns and these glycans are binding sites for lectins, hence lectins could be used as carrier molecules targeting drugs to specific cells.

We have cloned and sequenced the gene of lectin-like protein from cDNA of rice. Lectin-like protein was over-expressed in *Escherichia coli* JM109 carrying plasmid pQE30 (QIAGEN) which contains an inserted *lectin-like gene*, and the 15.2 kDa protein was purified using nickel-chelate chromatography. The protein crystals have been obtained and belong to the hexagonal symmetry with unit cell dimensions  $a = 97.90 \text{ \AA}$ ,  $b = 97.90 \text{ \AA}$ , and  $c = 44.85 \text{ \AA}$ . The structure determination of lectin-like protein is in progress.

Shell		I/Sigma in resolution shells:									
Lower limit	Upper limit	0	1	2	3	5	10	20	>20	total	
30.00	3.96	0.1	0.2	0.3	0.4	0.4	0.8	4.8	85.8	90.6	
3.96	3.15	0.0	0.1	0.2	0.3	0.6	1.1	4.6	94.2	98.8	
3.15	2.75	0.1	0.5	1.0	1.6	2.4	5.6	13.2	85.9	99.1	
2.75	2.50	0.5	1.5	3.0	4.3	7.5	16.2	38.9	60.3	99.2	
2.50	2.32	1.2	3.0	4.5	7.0	13.0	25.9	57.1	41.1	98.2	
2.32	2.18	1.9	4.4	8.3	12.4	20.7	41.6	81.4	16.6	98.0	
2.18	2.07	2.2	6.3	11.7	18.3	31.0	56.8	91.8	6.3	98.1	
2.07	1.98	2.6	8.4	17.2	28.9	48.2	77.4	97.9	0.0	97.9	
1.98	1.91	6.6	17.7	31.7	44.9	63.8	87.5	98.1	0.0	98.1	
1.91	1.84	18.3	34.7	49.7	62.7	77.6	92.7	97.1	0.0	97.1	
All hkl		3.3	7.6	12.6	17.9	26.2	40.1	58.0	39.5	97.5	

Summary of reflections intensities and R-factors by shells  
 R linear =  $\text{SUM}(|\text{ABS}(I - \langle I \rangle)|) / \text{SUM}(I)$   
 R square =  $\text{SUM}(|I - \langle I \rangle|^2) / \text{SUM}(I^2)$   
 Chi<sup>2</sup> =  $\text{SUM}(|I - \langle I \rangle|^2) / (\text{Error}^2 * N / (N-1))$   
 In all sums single measurements are excluded

Shell limit	Lower limit	Upper limit	Average I	Average I error	Stat. Chi <sup>2</sup>	Norm. R-fac	Linear R-fac	Square R-fac
30.00	3.96	46700.8	1507.4	1146.6	3.969	0.022	0.028	
3.96	3.15	22469.3	657.7	414.6	2.443	0.024	0.028	
3.15	2.75	6332.6	185.4	112.1	2.374	0.029	0.031	
2.75	2.50	2400.7	100.1	96.6	2.531	0.035	0.039	
2.50	2.32	1355.2	67.9	67.9	0.000	0.000	0.000	
2.32	2.18	867.6	59.3	59.3	0.000	0.000	0.000	
2.18	2.07	575.6	51.9	51.9	0.000	0.000	0.000	
2.07	1.98	345.9	48.5	48.5	0.000	0.000	0.000	
1.98	1.91	220.0	43.5	43.5	0.000	0.000	0.000	
1.91	1.84	118.0	39.9	39.9	0.000	0.000	0.000	
All reflections		8088.7	274.3	206.5	2.855	0.023	0.028	